Stretch to See: Lateral Tension Strongly Determines Cell Survival in Long-Term Cultures of Adult Porcine Retina

Linnéa Taylor,[1] *Damian Moran,*[2] *Karin Arnér,*[1] *Eric Warrant,*[2] *and Fredrik Ghosh*[1]

Purpose. To explore the effect of lateral tension as a survival factor for retinal explants in vitro. The central nervous system (CNS) resides in a highly mechanical milieu. However, the importance of biomechanical homeostasis for normal CNS function has not been extensively explored. Diseases in which normal mechanical forces are disrupted, such as retinal detachment of the eye, are highly debilitating and the mechanisms underlying disease progression are not fully understood.

Methods. Using a porcine animal model, we developed a novel technique of culturing adult retinal explants under stretch for up to 10 days in vitro (DIV). These were compared with standard (no stretch) and free-floating cultured explants. Cell survival was analyzed using immunohistochemistry, and retinal architecture using hematoxylin and eosin staining.

Results. Compared with unstretched specimens, which at 10 DIV degenerated into a gliotic cell mass, stretched retinas displayed a profound preservation of the laminar retinal architecture as well as significantly increased neuronal cell survival, with no signs of impending gliosis.

Conclusions. The results confirm that biomechanical tension is a vital factor in the maintenance of retinal tissue integrity, and suggest that mechanical cues are important components of pathologic responses within the CNS. (*Invest Ophthalmol Vis Sci.* 2013;54:1845–1856) DOI:10.1167/iovs.12-11420

The eye is under constant influence from external and internal mechanical forces.[1] To maintain visual function under various conditions, the ocular tissues thus must display a high degree of structural integrity as well as biomechanical adaptability. The highly delicate neural retina is composed of neurons embedded within a framework of Müller glia cells, forming a transparent sheet held in place between the vitreous cortex and the retinal pigment epithelium (RPE). The biomechanical properties of the retina have been described to some extent, including characterization of elasticity and tensility of the intact tissue as well as of individual glial and neuronal elements.[2–7] The retinal tissue is known to adapt mechanically to changes during development, where radical stretch of the retina during expansion of the globe is enabled by an increased elastic modulus.[3] This stretched state is maintained in the adult eye by the intraocular pressure (IOP) and photoreceptor–RPE adhesion.[8,9]

The importance of retinal tension for retinal tissue integrity and function is a topic that has not been widely explored. However, conditions exist when normal tension is lost such as rhegmatogenous retinal detachment (RRD), which occurs in the human eye when vitreous-derived fluid separates the retina from the RPE. The consequences of RRD include activation, stiffening, and remodeling of Müller glia, loss of photoreceptor function, and neuronal destabilization in inner retinal layers, phenomena that so far have not been fully explained.[10–14]

To simulate loss of retinal tension in vitro, retinal explants can be isolated from its surrounding tissues and from the influence of the IOP.[13] Traditionally, retinal tissue is maintained in standard tissue culture dishes with artificial cerebrospinal fluid media and minimal tissue support provided by a culture membrane. Adult retina under these conditions shows poor survival, with widespread neuronal cell death after 3 to 4 days.[15–19] As in retinal detachment in vivo, the degeneration of retinal neurons in vitro is preceded by rapid activation of the Müller cells. Neuronal degeneration and gliosis are thus hallmarks of the isolated adult retina in vitro and, as such, this model is well suited for study of factors that influence retinal homeostasis.

Here we hypothesized that lateral tension is an important factor for cell survival and tissue integrity within the retina. To test this, we developed a novel culturing technique that stretches the explanted retina as well as prevents gliosis-induced shrinkage of the retinal tissue, and we compared such tissue with retinas kept under traditional conditions. Our results indicate that retinal tissue tension is indeed important for cell survival, and that a moderate degree of stretch preserves retinal architecture for at least 10 days in vitro (DIV), with enhanced survival of photoreceptors and ganglion cells, as well as an attenuation of glial activation. These findings are not only important for advancing long-term organotypic culture of the retina, but also offer insights into the pathologies that originate from perturbation of the biomechanical milieu of the eye, such as retinal detachment.

Materials and Methods

Tissue Culturing

All proceedings and animal treatments were in accordance with the guidelines and requirements of the Committee on Animal Experimentation at Lund University and with the ARVO statement on the use of animals in ophthalmic and vision research. Eyes were harvested from adult pigs aged between 4 and 6 months, euthanized by an overdose of sodium pentobarbital (Apoteket, Umeå, Sweden). The neuroretinas were removed using the method described previously by Engelsberg and Ghosh in 2007.[17] To summarize, the eyes were enucleated

From the [1]Department of Ophthalmology, Lund University Hospital, Lund, Sweden; and the [2]Department of Biology, Lund University, Lund, Sweden.

Supported by The Faculty of Medicine, Lund University, The Swedish Research Council; The Princess Margaretas Foundation for Blind Children; and the Marianne and Marcus Wallenbergs Foundation.

Submitted for publication December 3, 2012; revised January 9, 2013; accepted January 23, 2013.

Disclosure: **L. Taylor**, None; **D. Moran**, None; **K. Arnér**, None; **E. Warrant**, None; **F. Ghosh**, None

Corresponding author: Linnéa Taylor, Department of Ophthalmology, Lund University Hospital, S-22184 Lund, Sweden; linnea.taylor@med.lu.se.

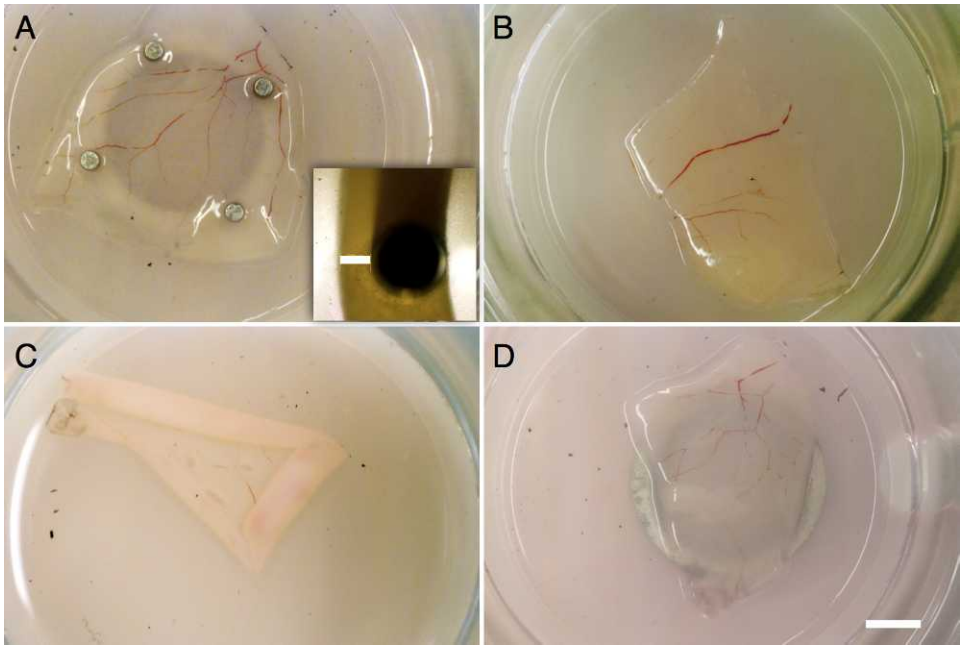

Figure 1. The four different culture settings. A stretched porcine retinal explant (**A**) using an NdFeB, Ni-plated ring magnet under the culture membrane, and four small disc magnets pinning the explant to the membrane. The *inset* shows the distance (*white bar*) the disc magnets could be moved on the ring magnet (seen under the culture membrane) to stretch the retinal explant. Standard culture (**B**) showing an explanted retinal section on a culture membrane. Retinal explant free-floating in culture medium (**C**). Magnet control culture (**D**) with an NdFeB, Ni-plated ring magnet under the culture membrane and the retinal explant placed on the membrane as in (**B**). *Scale bar*: 20 mm.

immediately after euthanization and immersed in CO_2-independent medium (Invitrogen, Paisley, UK). The anterior segment was removed by a sharp incision in the pars plana and cut 360°. The neuroretinas were removed by gentle dissection from the pigment epithelium with microforceps and cutting at the optic nerve head. Each neuroretina was sectioned into three pieces so that each piece had a central, cone-dense part. Each specimen measured approximately 12 to 15 mm^2. In total, 31 eyes from 16 animals were used, yielding 73 specimens for culture and six eyes serving as in vivo reference specimens. The 73 neuroretinal pieces were explanted onto 0.4-μm culture-plate inserts (Millicell-PCF; Millipore, Billerica, MA), with the photoreceptors facing the membrane. The membrane is porous to allow for nutrient diffusion to the tissue from the medium. Specimens were cultured in 1.5 mL (stretch and standard cultures) or 3 mL (free-floating cultures) Dulbecco's modified Eagle's medium/nutrient mixture F12 (DMEM/F12; Invitrogen) supplemented with 10% fetal calf serum (Sigma-Aldrich, St. Louis, MO) and maintained at 37°C at 95% humidity and 5% CO_2. The medium was exchanged every second day.

The explants were divided into three main culture groups (Fig. 1). Group 1 ($n = 32$ explants) was cultured in a stretched state, where a ring magnet was placed under the culture membrane at the bottom of the culture well, with the explanted retina positioned on the membrane so that the central part was placed over the ring magnet center. The ring magnet measured 12 and 9 mm, external and internal diameter, respectively. Four small disc magnets (∅ 1 mm) were then used to pin the edges and stretch the flattened retina on the culture membrane to the ring magnet underneath (Fig. 1A). Disc and ring magnets were made of neodymium (NdFeB), Ni-plated with a magnetic strength of 1.32 to 1.37 Tesla (Supermagnete; Webcraft GmbH, Gottmadingen, Germany). Metal foreceps were used to place the small disc magnets on the inner part of the ring magnet, and the small magnets were then pushed out radially using the foreceps, so that the retina was stretched. When the small disc magnets were positioned, holes in the explant were created where they were placed, and could thereby stretch the retina without producing increased adhesion to the culture membrane. The stretch of the retina was approximately 7% based on the distance the small disc magnets were moved in relation to the inner diameter of the ring magnet (Fig. 1A, inset). This level of stretch was chosen based on earlier findings regarding the elasticity, plasticity, and breaking point of the porcine retina.[5] A drop of culture membrane was added on top of the explant to prevent drying out of the tissue.

Group 2 ($n = 14$) was cultured under standard conditions (unstretched), as previously described by Engelsberg and Ghosh in 2007,[17] where the retinal explant was placed on the outer nuclear layer (ONL) down on the membrane, with a drop of culture medium on top to prevent drying of the tissue (Fig. 1B).

Group 3 ($n = 14$) was cultured free-floating in culture medium (Fig. 1C).

Explants were fixed at 2, 5, and 10 DIV.

Magnet controls ($n = 13$) were also performed to isolate any effects from the metal or magnetic field. This treatment was the same as the standard cultures, except for the addition of a ring magnet under the culture membrane (Fig. 1D).

Histology

Histologic examinations were performed as described by Engelsberg and Ghosh in 2007,[17] and are summarized as follows. After culturing, the explants were fixed in 4% paraformaldehyde in 0.1 M phosphate buffer, pH 7.2 for 2 hours at 4°C. The in vivo reference specimens were fixed immediately after harvest using the same paraformaldehyde concentration for 4 hours at 4°C. The explants were then infiltrated with 0.1 M Sörensen's medium with increasing concentrations of sucrose up to 25%. They were then embedded with the culture membrane in egg albumin/gelatin medium for cryosectioning at −20°C, with a section thickness of 12 μm. For light microscopy, every tenth slide was stained with hematoxylin and eosin. For immunohistochemical labeling, adjoining slides with sections originating from the center of the explants (the area centralis in the normal control) were chosen. The specimens were rinsed three times with PBS containing 0.1% Triton X-100, and then incubated with PBS containing 0.1% Triton X-100 and 1% bovine serum albumin (BSA) for 20 minutes at room temperature. After this, specific retinal cell types were labeled in individual specimens using one of a number of different antibodies (see the Table

Table. Primary and Secondary Antibodies Used for Immunohistochemical Analysis

Antigen	Antibody Name	Target Cell	Species	Dilution	Source	Reference
Primary antibody						
NeuN	Antineuronal nuclei	Ganglion cells, displaced amacrine cells	Mouse monoclonal	1:100	Millipore, Billerica, MA	20
Vimentin	Mouse antivimentin	Müller cells	Mouse monoclonal	1:500	Chemicon International, Temecula, CA	20
Rhodopsin	Rho4D2	Rod photoreceptor	Mouse monoclonal	1:100	Kind gift of Robert S. Molday, PhD, Vancouver, Canada	49
GFAP	Antiglial fibrillary acidic protein	Activated Müller cells, astrocytes	Mouse monoclonal	1:200	Chemicon International	20
Secondary antibody						
FITC	Antimouse IgG FITC conjugate	Antimouse	Goat	1:200	Sigma-Aldrich, St. Louis, MO	49

for details). This was achieved by incubating the specimens overnight at 4°C with the respective primary antibody (Table). The specimens were then rinsed in PBS–Triton X-100 (0.1%), and incubated for 45 minutes with a secondary fluorescein isothiocyanate (FITC; Table), and then mounted in mounting medium with 4′,6-diamidino-2-phenylindole (DAPI) (Vectashield; Vector Laboratories Inc., CA). Negative control experiments were performed as above, replacing the primary antibody with PBS containing 0.1% Triton X-100 and 1% BSA. In vivo reference specimens were used as positive controls. Photographs were taken using an epifluorescence microscope (Eclipse E800; Nikon, Tokyo, Japan) equipped with a digital acquisition system (DP 70; Olympus, Tokyo, Japan). The ×40 objective was used to acquire images.

Terminal deoxynucleotidyl transferase dUTP nick end labeling (TUNEL) staining was performed (TMR red In Situ Cell Death Detection kit; Roche Diagnostics GmbH, Mannheim, Germany).

Statistical Analysis

Immunohistochemically labeled sections were used to statistically quantify survival of individual cell types. One central section per cultured specimen was analyzed for TUNEL, rhodopsin, and NeuN labeling, along with one section per in vivo reference eye. In vivo reference tissue and cultured specimens were processed in the same batch for each immunohistochemical labeling. Three photographs were obtained from the sections, and labeled cells (TUNEL and NeuN) and labeled cell rows in the ONL (rhodopsin) were counted at ×40 magnification. Normal control tissue and cultured specimens were processed in the same batch for each immunohistochemical labeling. Data were analyzed using ANOVA with a post hoc test (GraphPad InStat; GraphPad Software, San Diego, CA). Raw data from cell counts were used to generate mean values for each of the groups. Values of $P < 0.05$ were considered significant.

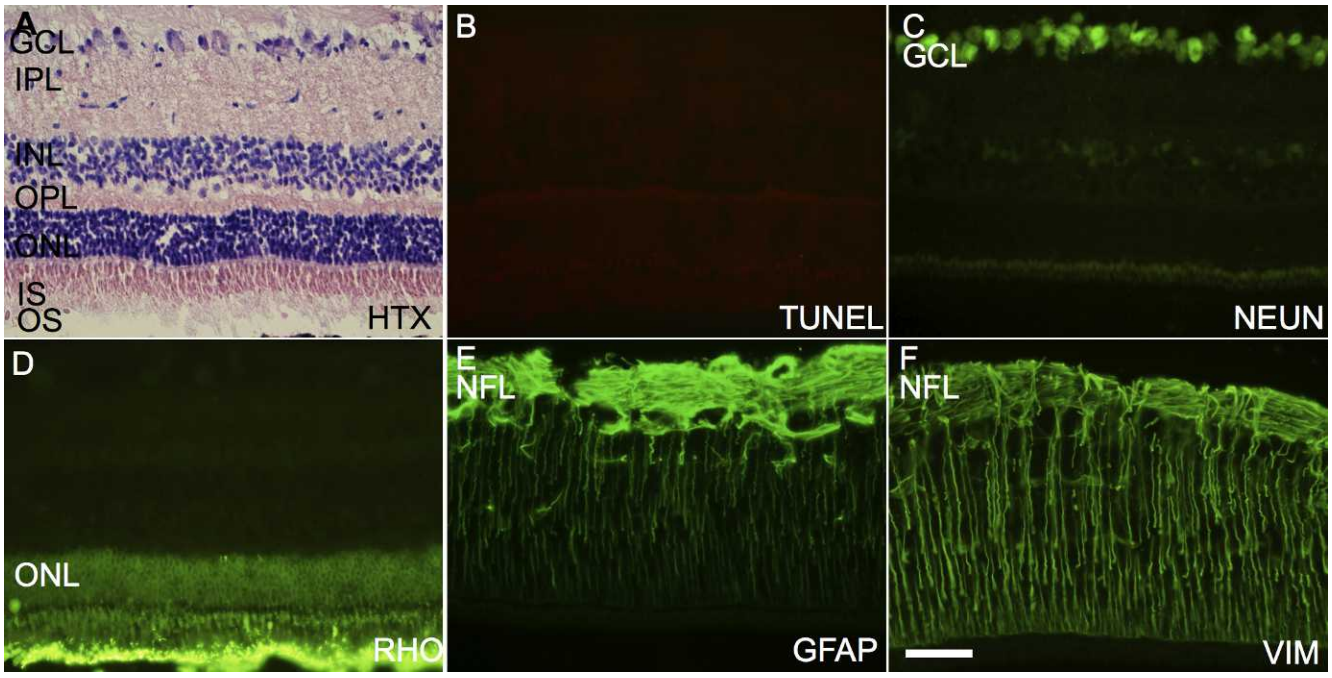

Figure 2. Normal adult porcine control retinas (in vivo controls). (**A**) Hematoxylin and eosin staining. (**B–H**) Immunohistochemistry. Hematoxylin and eosin staining (**A**) show normal, well-populated nuclear layers with normal retinal lamination. TUNEL labeling shows no labeled cells (**B**). NeuN-labeling (**C**) shows large cells of ganglion morphology localized to the GCL. Outer segments of rod photoreceptors are strongly labeled with rhodopsin (**D**). Inner segments and cell perikarya are more weakly labeled. Activated Müller cells are labeled with GFAP (**E**). A species-normal upregulation of GFAP in the Müller cell end feet can be seen in the NFL. Vimentin labeling shows numerous Müller cell fibers spanning the vertical length of the specimen (**F**). Some horizontal fibers are seen in the NFL. *Scale bar*: 50 μm.

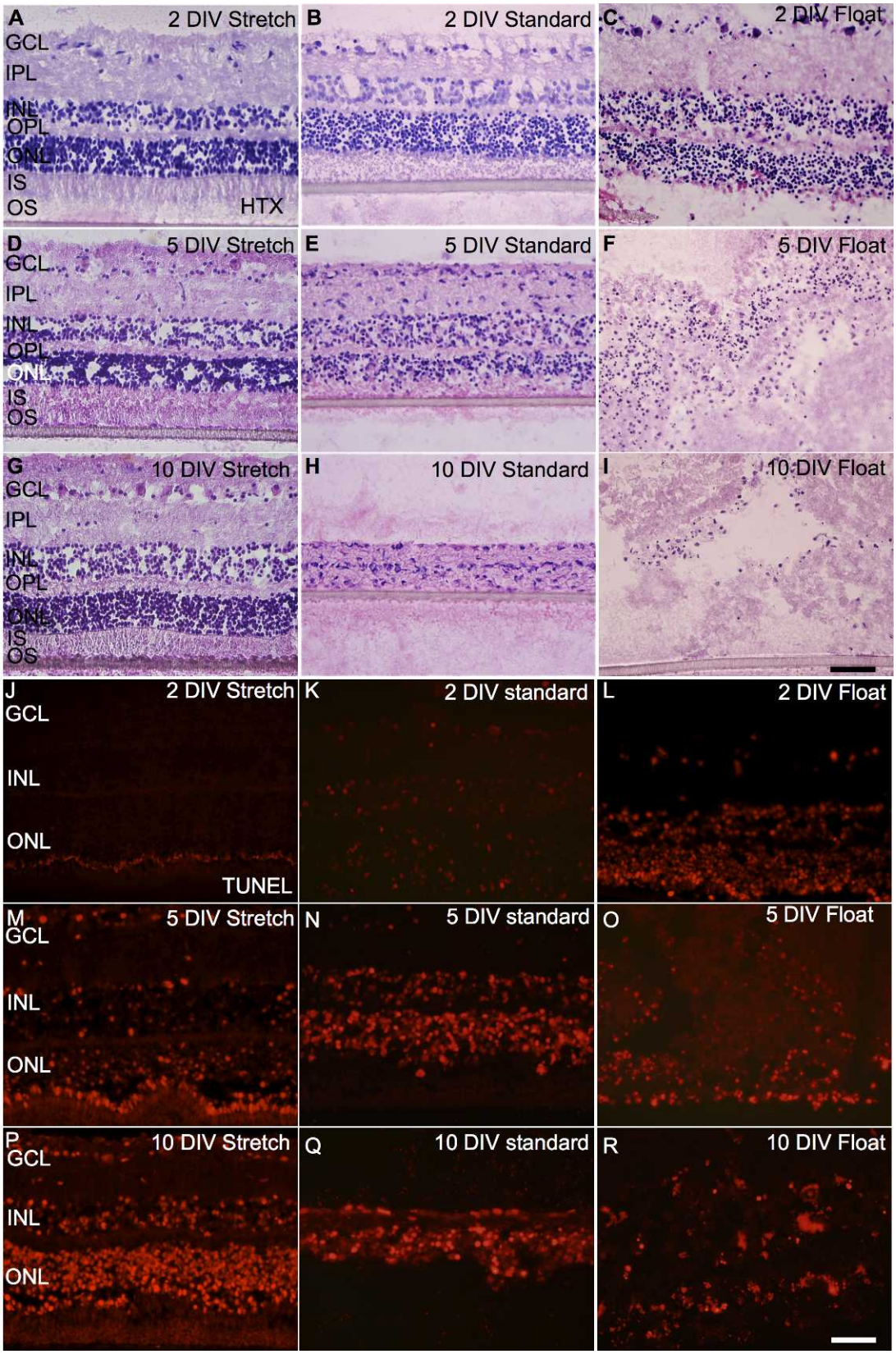

Figure 3. Hematoxylin and eosin staining (HTX/EOSIN) and TUNEL labeling of stretched, standard, and float-cultured explants at 2, 5, and 10 DIV. HTX/EOSIN staining of explants cultured for 2 DIV show that stretch-cultured explants (**A**) retain a normal laminated appearance with few pyknotic cells. Inner and outer segments are present, albeit slightly disorganized (**B**). Standard-cultured specimens display an overall thinning as well as numerous pyknotic cells, mainly localized to the ONL. Inner and outer segment debris are present in the outer part of the specimen. Free-floating cultured specimens show dissolving retinal lamination, with most cells appearing pyknotic (**C**). 5 DIV stretch-cultured explants have maintained the laminar organization seen in 2 DIV cultures (**D**). Inner and outer segments are present, although they appear disorganized. Standard-cultured

specimens at the same time point show dissolving retinal layers with numerous pyknotic cells in all cell layers, and appear thinner than stretched cultures (**E**). Specimens cultured free-floating display an overall loss of retinal architecture with no discernible cell layers (**F**). Most cells appear pyknotic. 10 DIV stretch-cultured explants retain the normal laminated morphology seen at 2 and 5 DIV (**G**). Disorganized inner and outer segments are present. The cultured membrane appears darkened by debris. Standard-cultured specimens display a complete loss of the normal laminar architecture with no discernible cell layers present (**H**). The specimens appear drastically thinner compared with stretch-cultured counterparts. Float-cultured explants at the same time point appear as a degenerated cell mass with few remaining cells (**I**). TUNEL labeling of 2 DIV stretch-cultured explants displays a monolayer of labeled cells at the outer border of the ONL (**J**). Corresponding standard and free-floating cultured explants show numerous TUNEL-positive cells in all cell layers (**K**, **L**). At 5 DIV, stretch-cultured explants retain the monolayer of labeled cells in the outer ONL seen at 2 DIV, but also display a scattering of labeled cells in all cell layers throughout the specimen (**M**). Standard-cultured explants at the same time point show a multitude of labeled cells in all cell layers (**N**). Free-floating cultures show numerous labeled cells throughout the specimen (**O**). At 10 DIV, stretch-cultured explants show TUNEL-positive cells in all cell layers (**P**). Correspondingly, all remaining cells in standard and free-floating cultured explants appear to be TUNEL positive (**Q**, **R**). *Scale bar*: 50 μm.

Results

In Vivo Reference Specimens

The morphology of porcine adult in vivo retina has already been described in detail,[23,24] but is of importance, and will therefore be briefly summarized. Hematoxylin and eosin staining of adult normal retina displayed well-defined nuclear layers, with larger cell bodies in the INL compared with the ONL (Fig. 2A). The inner plexiform layer (IPL) was several times wider than the outer plexiform layer (OPL). The ganglion cell layer (GCL) displayed a monolayer of large retinal ganglion cell (RGC) bodies and smaller displaced amacrine cells. The nerve fiber layer (NFL) was significantly thinner in the periphery compared with central sections. TUNEL labeling showed no labeled cells (Fig. 2B). In immunohistochemically labeled sections, the NeuN antibody mainly labeled large cell bodies in the GCL corresponding to ganglion cells (Fig. 2C). Rhodopsin labeling of rod photoreceptors displayed the strongest intensity in outer segments, with weaker cytoplasmic labeling of inner segments and nuclei in the ONL (Fig. 2D). Glial fibrillary acidic protein (GFAP) was used to label activated Müller cells. Weakly labeled vertically arranged structures corresponding to Müller cells were found spanning most retinal layers (Fig. 2E). In the innermost part, labeling was very strong, corresponding to horizontal Müller cell fibers as well as astrocytes. This labeling is normal for this species.[20] Vimentin labeling was used to label Müller cells (Fig. 2F). The Müller cell fibers were visible as well-organized vertical structures spanning the retina from the NFL to the outer layers.

Cultured Adult Explants

Hematoxylin and Eosin Staining. Stretched cultures displayed a normal, layered retinal architecture at 2 DIV, with small vacuoles in the nuclear layers (Fig. 3A). Photoreceptor inner and outer segments were present, albeit slightly disorganized. Standard cultures at the same time point displayed pyknotic cells in all cell layers, most prominently in the ONL (Fig. 3B). The outer segment layer of these specimens contained no normal outer segments, but were filled with debris. The overall thickness of the specimens was decreased compared with the stretched cultures at the same time point. Floating explants appeared curled and shrunken as well as edematous, and with a dissolving retinal architecture in which the majority of cells were pyknotic (Fig. 3C). At 5 DIV, the stretched specimens displayed a laminated morphology comparable with 2 DIV counterparts (Fig. 3D). Pyknotic cells were more abundant in all cell layers. Inner and outer segments were present but slightly disorganized. In the standard 5 DIV cultures, the retinal layers appeared to be dissolving (Fig. 3E). The ONL and INL contained fewer cells than 2 DIV counterparts, and the majority appeared pyknotic. The 5 DIV floating cultures (Fig. 3F) displayed an almost complete dissolution of the retinal architecture in which no layers could be discerned. All cells appeared pyknotic, and the tissue was edematous. The 10 DIV stretched cultures retained the laminated morphology seen at 2 and 5 DIV (Fig. 3G). Inner segments were present, but outer segments were disorganized and a thin layer of debris was seen attached to the culture membrane. The specimens cultured under standard conditions had completely lost the normal laminated appearance and were markedly thinner than their stretched counterparts (Fig. 3H). Very few cells were present, and no inner or outer segments could be found. The 10 DIV floating cultures (Fig. 3I) had degenerated almost completely.

TUNEL. In 2 DIV stretch-cultured specimens, one row of TUNEL-labeled cells was found in the outermost part of the ONL (Fig. 3J). No labeling was present elsewhere. Standard and floating explants displayed numerous labeled cells in all cell layers (Figs. 3K, 3L). Statistical analysis showed no significant difference in the number of TUNEL-labeled cells between stretched and standard cultured explants (Fig. 4a). Explants cultured free-floating displayed a significantly higher number of labeled cells ($P < 0.001$). At 5 DIV, the specimens cultured under stretch (Fig. 3M) displayed scattered labeled cells in all nuclear layers, but retained a band of positively labeled cells in the outer ONL. The specimens cultured under standard conditions contained numerous TUNEL-positive cells in all cell layers (Fig. 3N). In floating explants, the majority of remaining cells were positively labeled (Fig. 3O). Statistical analysis revealed that a significantly higher number of cells were found to be TUNEL positive in specimens cultured under standard conditions compared with stretch-cultured explants (Fig. 4a; $P < 0.05$). No significant difference in the number of labeled cells was found comparing the stretched cultures to floating explants. In 10 DIV specimens of all groups, the remaining cells were TUNEL positive (Figs. 3P–R). Statistical analysis showed that stretched explants displayed a significantly higher number of TUNEL-positive cells in comparison to standard and floating cultured specimens (Fig. 4a; $P < 0.001$).

NeuN. NeuN labeling of 2 DIV stretched cultures displayed numerous labeled cells in the GCL with an appearance consistent with ganglion cells (Fig. 5A). In comparison, specimens cultured under both standard (Figs. 4b, 5B; $P < 0.01$) and free-floating (Figs. 4b, 5C; $P < 0.001$) conditions displayed few scattered labeled cells in the GCL of a ganglion cell morphology. At 5 DIV, stretch-cultured specimens retained a large number of labeled cells of ganglion cell morphology in the GCL (Fig. 5D). The standard-cultured specimens displayed a similar number of labeled cells in the GCL to that observed at 2 DIV, as well as scattered structures in the IPL (Fig. 5E). In contrast, the free-floating explants displayed very weakly labeled cells scattered throughout the specimen in a seemingly random fashion (Fig. 5F). The stretch-cultured explants showed a significantly higher number of NeuN-labeled cells when compared with free-floating cultures ($P < 0.001$), but no significant difference could be found when compared with the standard culture group. At 10 DIV, stretched specimens

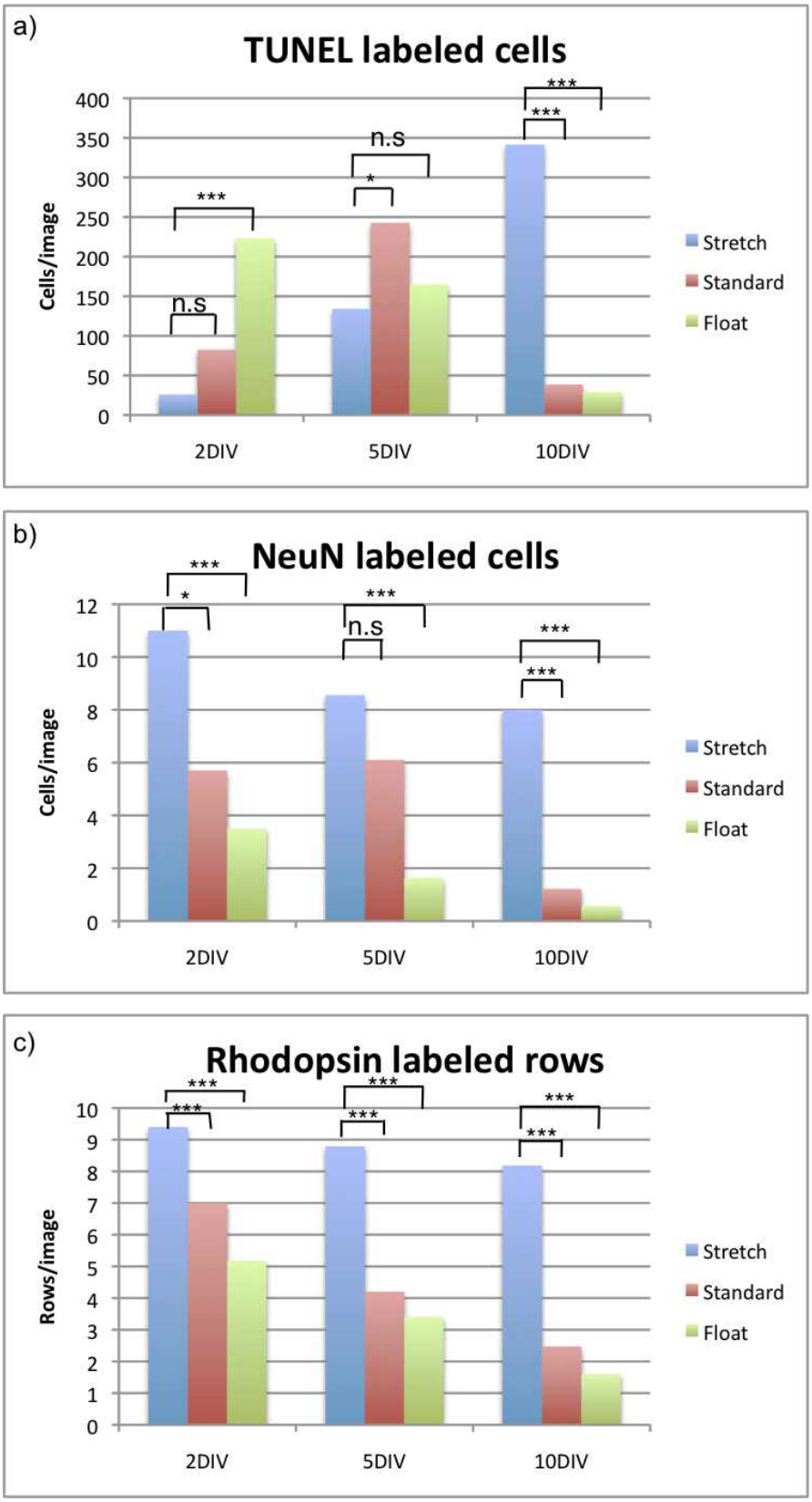

Figure 4. Diagrams of changes in TUNEL- and NeuN-labeled cells as well as rhodopsin-labeled rows over time. (**a**) TUNEL-labeled cells. (**b**) NeuN-labeled cells. (**c**) Rhodopsin-labeled rows. Stretch cultures show an increase in the number of TUNEL-labeled cells over time, whereas free-floating cultured explants peak at 2 DIV and then show a decrease in the number of labeled cells, and standard cultured explants peak at 5 DIV (**a**). The number of NeuN-labeled cells rapidly declines after 2 DIV in free-floating cultures, whereas the stretch-cultured group shows a slower decline over time (**b**). The standard cultures show a low but constant number of NeuN-labeled cells at 2 and 5 DIV, with a significant drop in number of cells at 10 DIV. The number of rhodopsin-labeled rows declines over time in all culture groups; however, the stretch cultures show a significantly slower rate of cell loss (**c**) (n.s., not significant; $^{*}P > 0.05$; $^{***}P > 0.001$).

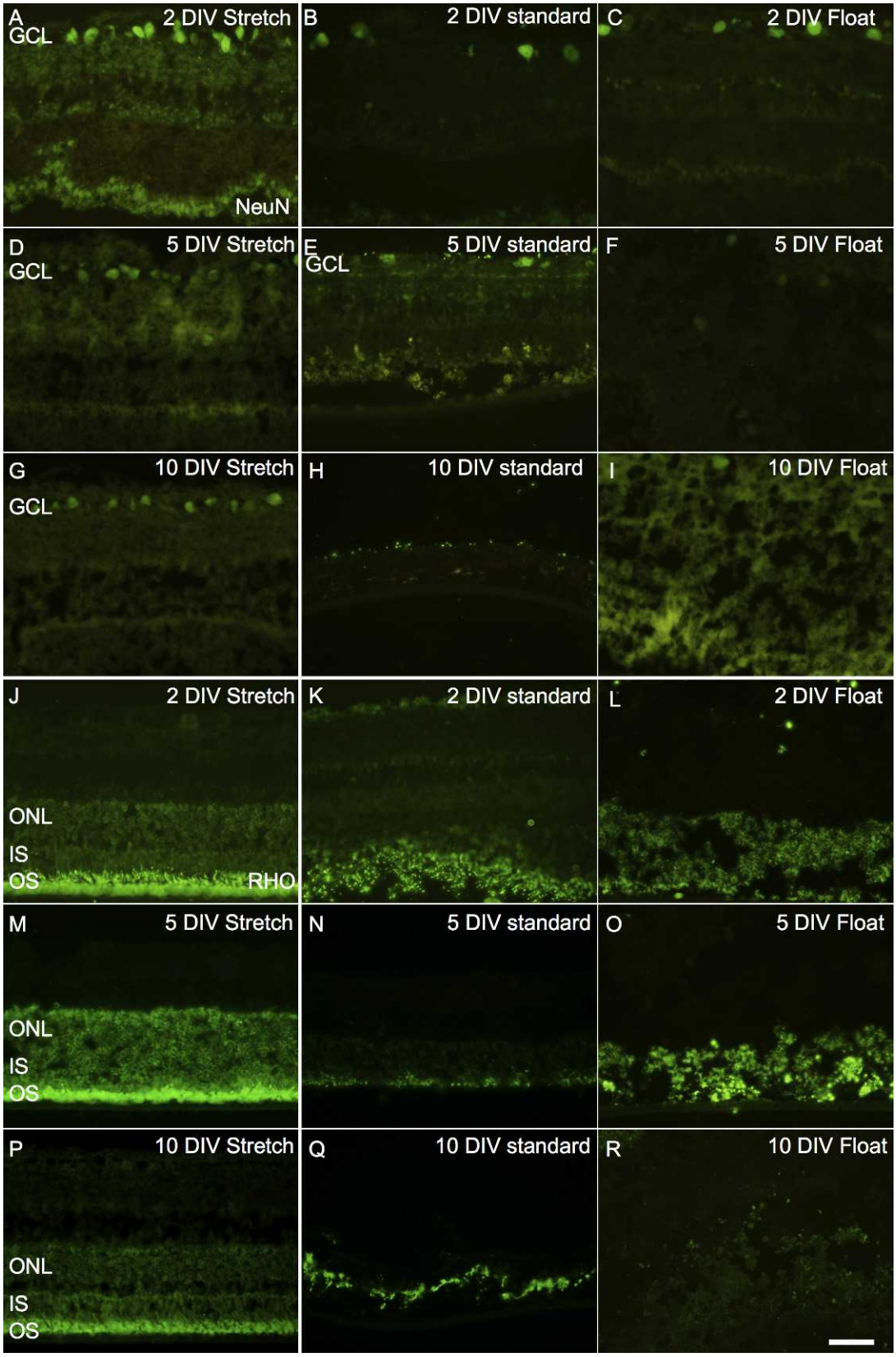

Figure 5. Immunohistochemical labeling of ganglion cells and rod photoreceptors using NeuN and rhodopsin. At 2 DIV, stretch-cultured explants show numerous NeuN-labeled cells of ganglion appearance in the GCL (**A**). Corresponding standard and free-floating culture specimens show scattered labeled cells in the GCL (**B**, **C**). At 5 DIV, stretch-cultured specimens display many labeled cells of ganglion cell appearance in the GCL (**D**). Standard cultures at the same time point show scattered labeled perikarya, as well as scattered structures in the inner part of the specimen (**E**). Free-floating cultures display very weak labeling of isolated cell-like structures located randomly throughout the specimen (**F**). At 10 DIV, stretch-cultured explants show many labeled cells in the GCL, although they appear to be fewer than at 2 and 5 DIV (**G**). Corresponding standard cultures show

strong labeling of unidentifiable structures at the inner border of the specimen (**H**). Specimens cultured free-floating show very few, isolated, weakly labeled cell-like structures at random locations in the specimen (**I**). Rhodopsin labeling of 2 DIV cultures revealed stretch-cultured explants as having well-preserved inner and outer segments as well as a clearly defined ONL (**J**). Standard-cultured specimens display strongly labeled remnants of outer segments in the outermost part of the specimen, as well as weakly labeled perikarya in the ONL (**K**). Free-floating cultured explants show strong labeling of cell bodies localized to the ONL, the overall morphology of which appears disrupted (**L**). At 5 DIV, stretch-cultured specimens show strong labeling of both rod cell bodies and inner and outer segments (**M**). Standard-cultured explants display very weak labeling of cell bodies in the ONL, with slightly stronger labeling of what appears to be remnants of photoreceptor inner and outer segments in the outermost part of the specimen (**N**). Free-floating cultured specimens show strong labeling of rod photoreceptor cell bodies in what appears to be a very disrupted ONL (**O**). At 10 DIV, stretch-cultured specimens show strong labeling of rod outer segments, with weaker labeling of inner segments and cell perikarya (**P**). Standard-cultured explants display labeling of disorganized structures in the outermost part of the specimen (**Q**). Free-floating cultures display labeling of small isolated structures scattered throughout the specimens (**R**). *Scale bar*: 50 μm.

displayed numerous labeled cells of a ganglion cell appearance in the GCL, albeit slightly fewer than those at 2 and 5 DIV (Fig. 5G). In comparison, very few labeled ganglion cells were present in the standard-cultured or floating specimens, and the sections showed labeling of scattered and unidentifiable structures at the inner border of the specimen (Figs. 4b, 5H, 5I; $P < 0.001$).

Rhodopsin. Rhodopsin labeling of specimens cultured under stretch for 2 DIV showed strong labeling of rod photoreceptor outer segments, as well as weak labeling of inner segments and perikarya in the ONL (Fig. 5J). Standard cultured specimens at the same time point showed labeling of degenerated inner and outer segments, as well as weak labeling of scattered cell bodies in the ONL (Fig. 5K). Specimens cultured free-floating for 2 DIV displayed strong labeling of rod photoreceptor perikarya in the disrupted ONL (Fig. 5L). Stretch-cultured specimens at 5 DIV showed very strong labeling of both inner and outer segments as well as of the entire ONL (Fig. 5M). Specimens cultured under standard conditions at 5 DIV displayed weak labeling of scattered structures in the outer part of the ONL (Fig. 5N). Specimens cultured floating in medium at the same time point showed strong labeling of scattered disorganized structures (Fig. 5O). At 10 DIV, stretch-cultured specimens displayed labeling of rod outer segments, with weaker labeling of inner segments and nuclei in the ONL (Fig. 5P). Specimens cultured under standard conditions showed a disorganized band of labeled structures (Fig. 5Q). Specimens cultured free-floating displayed a myriad of small labeled structures throughout the specimens (Fig. 5R). At all time points, stretched cultures displayed a significantly higher number of rhodopsin-labeled rows compared with all other culture groups ($P < 0.001$; Fig. 4c).

GFAP. GFAP labeling of 2 DIV stretch cultures showed weak labeling of scattered Müller cell fibers vertically spanning the inner layers (Fig. 6A). Standard cultures of 2 DIV displayed strong GFAP labeling in the inner half of the specimen, with some areas of weaker labeling in the outer part (Fig. 6B). The labeled Müller cells appeared hypertrophied and slightly disorganized. Explants cultured free-floating showed scattered areas of strong labeling in the inner part of the specimen (Fig. 6C). Labeled Müller cells appeared disorganized. At 5 DIV, stretched cultures showed strong GFAP labeling at the innermost part of the specimen, with weak labeling of scattered vertical fibers (Fig. 6D). Standard cultured specimens at the same time point displayed strong labeling of hypertrophied Müller cells (Fig. 6E). Specimens cultured free-floating displayed labeling of a few scattered, disorganized fibers (Fig. 6F). Stretch-explants, cultured for 10 DIV, showed GFAP labeling of well-organized vertical fibers (Fig. 6G). Standard cultures of 10 DIV displayed strongly labeled hypertrophic fibers of random organization (Fig. 6H). Free-floating cultures showed scattered labeling of unidentifiable structures (Fig. 6I).

Vimentin. Stretch and standard cultures of 2 DIV showed strong vimentin labeling of thin, well-organized Müller cell fibers vertically spanning the specimen (Figs. 6J, 6K). Free-floating cultures showed similar strong labeling of vertical Müller cell fibers in the inner part of the specimen, with weaker labeling in the outer part (Fig. 6L). At 5 DIV, stretch cultures showed labeling similar to that at 2 DIV (Fig. 6M). Standard cultures showed strong labeling of short, hypertrophied Müller cell fibers that vertically span the specimen (Fig. 6N). Explants cultured free-floating displayed strong labeling of scattered, disorganized fibers (Fig. 6O). Stretch-cultured explants showed strong labeling of Müller cell fibers, similar to that observed at 5 DIV (Fig. 6P). Standard-cultured explants at the same time point display strong labeling of short, hypertrophied Müller cells organized in a random fashion across the specimen (Fig. 6Q). Free-floating explants show strong labeling of random structures scattered throughout the specimen. No continuous fibers could be found (Fig. 6R).

Magnet Controls

The specimens cultured under standard conditions, but with a ring magnet placed in the culture tray, displayed distinctly more pyknotic cells and vacuoles in all nuclear layers at all time points compared with stretched cultured explants (not shown). Compared with specimens kept under standard conditions but without a magnet, the laminar organization of the explants was somewhat better retained. TUNEL labeling as well as immunohistochemistry of rod photoreceptors and ganglion cells revealed a low cell survival rate. After 10 DIV, all remaining cells appeared TUNEL positive, no NeuN-labeled cells could be found, and few isolated nuclei were weakly labeled with rhodopsin (not shown).

Discussion

In this study, we set out to investigate the influence of biomechanical environment on cell survival. Mechanical tension has been found to regulate cell survival in human bladder smooth muscle cells in vitro,[21] although to our knowledge, the concept of mechanical sensitivity as a factor for cell survival within the adult CNS has not been previously explored.

Using a novel organotypic culture technique that allows full-thickness retinal explants to be stretched, we observed not only an increased photoreceptor and ganglion cell survival, but also a preservation of the retinal architecture, with no signs of impending gliosis. This new culture method significantly expands the opportunities to study the retina in vitro as well as strengthens the notion that lateral tension is an important factor in the maintenance of a healthy retina.

Like the brain, the mechanical properties of the retina depend largely on neuronal cell bodies, nerve fiber bundles, and Müller cell end feet.[7] These elements are inhomogeneously distributed in the central-to-peripheral retina, resulting in differential viscoelastic properties.[3] During embryonic development of the eye, the retinal sheet becomes increasingly more elastic and stretched, especially in the periphery. These differences in viscoelasticity contribute to the development of

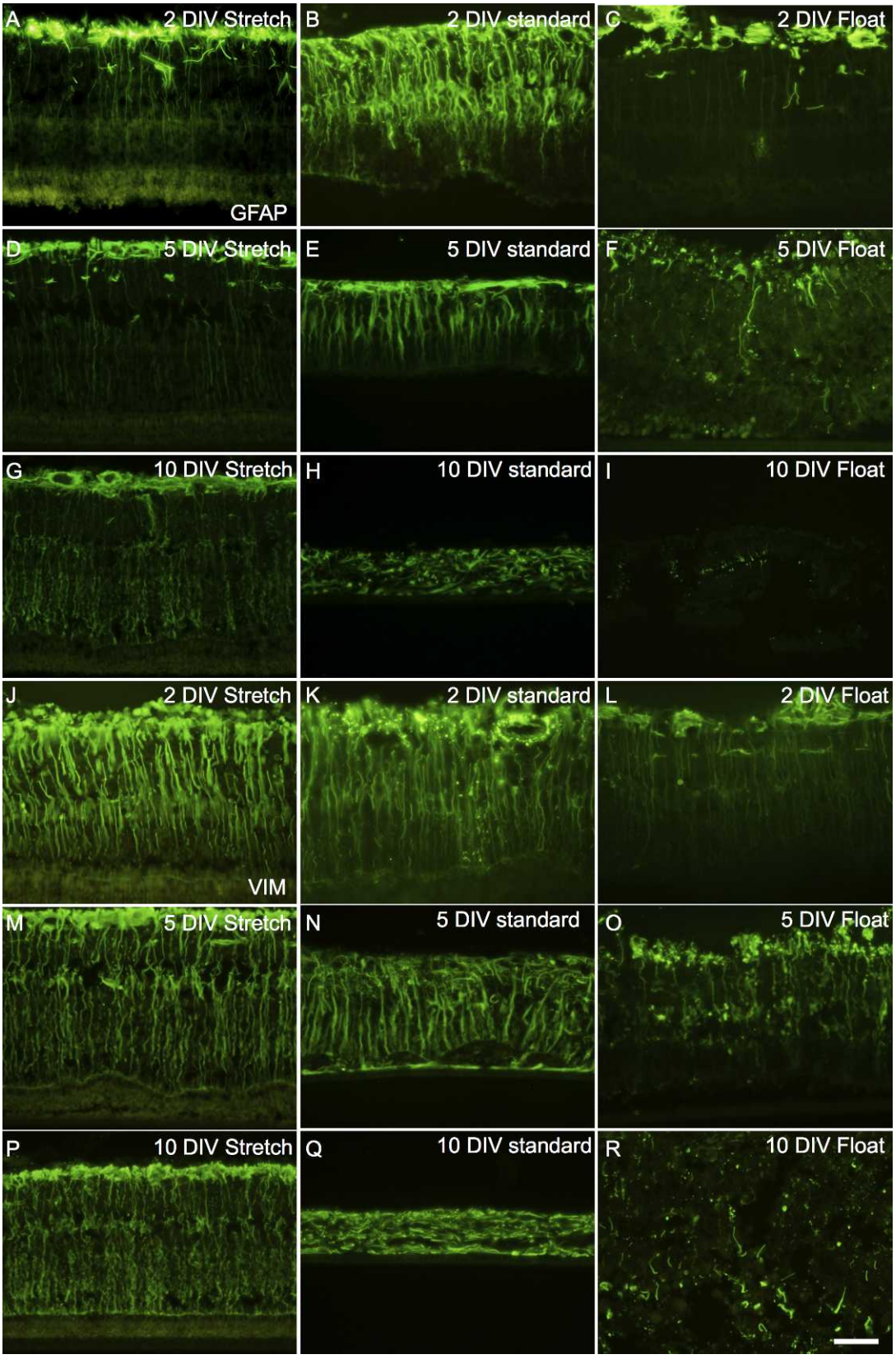

Figure 6. Immunohistochemical labeling of Müller cells using GFAP (activated cells) (**A–I**) and vimentin (**J–R**). At 2 DIV, stretch-cultured explants display strong GFAP labeling at the Müller cell end feet with weaker labeling of vertical fibers in the inner part of the specimen (**A**). The standard-cultured counterparts show strong labeling of thick and disorganized Müller cell fibers in the inner parts, with some labeled fibers spanning the entire specimen (**B**). Free-floating cultured explants show strong labeling of horizontal fibers at the innermost part of the specimen, with occasional vertical fibers labeled in the inner part (**C**). At 5 DIV, stretched cultures retain the labeling pattern seen at 2 DIV (**D**). The standard-cultured explants display strong labeling of short, thick Müller cell fibers spanning the vertical length of the specimen (**E**). Free-floating cultured specimens show

strong labeling of a few thin, disorganized fibers as well as some unidentifiable structures in the inner part of the specimen (**F**). At 10 DIV, stretch-cultured explants show strong labeling at the Müller cell end feet as well as weak labeling of thin, slightly disorganized vertical fibers (**G**). Standard-cultured counterparts show strong labeling of short and thick Müller cell fibers lacking any normal organization (**H**). Specimens cultured free-floating show labeling of small, unidentifiable structures scattered throughout the specimen (**I**). At 2 DIV, vimentin-labeling of stretch-cultured explants shows strongly labeled Müller cell fibers vertically spanning the specimen, terminating in the outer limiting membrane (**J**). Standard-cultured counterparts show a labeling pattern similar to that of the stretched cultures, albeit with slightly stronger labeling at the Müller cell end feet, as well as the fibers appearing slightly disorganized (**K**). Free-floating cultured explants show patches of strong labeling at the Müller cell end feet, as well as weak labeling of vertical fibers (**L**). At 5 DIV, stretch-cultured explants show slightly weaker labeling than that seen at 2 DIV, and the fibers appear slightly thinner (**M**). Corresponding standard-cultured explants display strong labeling of short and thick Müller cell fibers, which appear disorganized and damaged in the inner part of the specimen (**N**). Free-floating cultured explants show strong labeling of the highly disorganized Müller cell end feet in the innermost part of the specimen, as well as a few vertical fibers and unidentifiable structures scattered throughout the specimen (**O**). At 10 DIV, stretch-cultured explants show much the same labeling pattern as that seen at 5 DIV, albeit with slightly shorter and more disorganized vertical fibers (**P**). The standard-cultured counterparts display strong labeling of short, thick, and randomly oriented Müller cell fibers (**Q**). Explants cultured free-floating show strong labeling of short and randomly oriented fibers scattered throughout the specimen (**R**). *Scale bar*: 50 μm.

regional specialization such as areas of high visual acuity and the orderly cellular mosaic.[3,22,23]

The full significance of prevailing retinal tension in the normal eye is largely unknown. However, further understanding may be provided by conditions in vivo and in vitro in which tensility is lost. In human retinal detachment (RD), the retinal stabilizing forces are taken out of play due to posterior vitreous detachment (PVD), retinal tear formation, and inflow of vitreous-derived fluid into the subretinal space. Subsequently, the detached retina loses its fixation to the RPE, becomes highly mobile, and is released into the vitreous space. Traditionally, retinal reactions to RD have been attributed to ischemia due to loss of choroidal nutritional supply. However, several of the pathologic processes progress, in spite of reattachment, also indicating other contributing factors.[24] On a cellular level, the most obvious reaction to detachment occurs in the radial glia of the retina, the Müller cells. Spanning the entire width of the retinal layers, the Müller cells constitute the physical scaffold on which retinal neurons are precisely organized. Müller cells are also responsible for several retinal functions in the maintenance of retinal homeostasis.[25] Following detachment, Müller cells upregulate production of the intermediate filaments, GFAP and vimentin, a phenomenon considered to be the hallmark of gliosis.[24] The gliotic response is coupled with a disruption of the normal homeostatic Müller cell functions, such as neurotransmitter recycling, retinal ion and water homeostasis, and neurotrophic support.[26–28] From a biomechanical point of view it is interesting to note that upregulation of intermediate filaments in the Müller cells results in increased retinal stiffness and is coupled with a remodeling of the glial network associated with changes in the retinal architecture such as folding and shrinkage.[29,30] Thus, the apparent loss of mechanical tension in the detached retina is compensated by an increased stiffness in the tissue, indicating that a regulatory mechanism of retinal viscoelastic properties may exist, possibly for the purpose of stabilizing the delicate neuronal retinal network.

Interestingly, explanted retina kept in culture has been found to react much like a detached retina.[13] Like in detachment in vivo, activated Müller cells upregulate intermediary filaments, inducing stiffening of the tissue as well as release of cytokines and intracellular stores of glutamate.[24,28,29] These effects already lead to profound neuronal cell death after 3 DIV, and rapid formation of a gliotic scar, phenomena that are also seen in vivo after prolonged retinal detachment.[17,28,31] Ganglion cells and photoreceptors appear to be particularly sensitive to trauma elicited by the explant procedure and the in vitro milieu.[19,32] This has largely been attributed to the fact that the culture procedure requires an axotomy of the ganglion cell axons and photoreceptors are separated from the RPE.

Paradoxically, our stretched retinal explants displayed no signs of Müller cell activation and a substantial survival of photoreceptors and ganglion cells even at 10 DIV. In contrast, standard cultured explants, as previously reported, appeared to consist mainly of hypertrophic Müller cells with upregulation of GFAP expression. Cultured Müller cells have previously been shown to display a 4-fold increase in extracellular matrix (ECM) genes, such as connective-tissue growth factor (*Ctgf*), tenascin C (*Tnc*), Collagen Ia1 (*Col1a1*), and Collagen IVa3 (*Col4a3*). These genes are associated with proliferative vitreoretinopathy, a well-known complication that develops after retinal detachment, and were expressed in Müller cells cultured on soft substrates designed to mimic the loss of tissue stiffness found in a detached retina.[33] In our floating cultures, the phenomenon of Müller cell activation and tissue disruption was most pronounced, indicating a direct relationship between the biomechanical milieu and explant cell survival.

In the retinal explant culture paradigm, nutritive support is provided by the serum-containing medium.[18,34–36] This protocol is well established and is used by most groups studying organ cultures of adult full-thickness porcine retina.[13,18,19,36] Thus, the biomechanical loss of tension without interference from lack of nutritional support can be studied in isolation. Under standard culture conditions, the isolated retinal full-thickness explanted sheet has lost much of its normal tension, but is supported to some extent by the culture membrane. Our free-floating explants without any physical tissue support, but with ample supply of medium, degenerated profoundly. This increase in liquid surrounding the explants may have other detrimental effects such as diluting locally produced growth factors; however, this principle also applies to potentially toxic tissue-derived compounds such as glutamate. Thus, dilution effects are unlikely to account for the level of degeneration seen in these cultures. Put together, this again strengthens the notion that tissue tensility is an influential factor for retinal homeostasis.

Magnet controls show an overall preservation of the retinal laminar morphology, but with a cell death pattern similar to that seen in standard cultures. This seemingly conflicting result is possibly a combination of factors. The lack of biomechanical support, as in standard cultures, is a likely cause of the low rate of cell survival. The relative maintenance of the overall retinal architecture may be explained by the effect of placing a conducting tissue in a strong magnetic field effect, altering the spatial location of proteins and ions in the culture and thereby disturbing the tissue remodeling seen in the standard culture group.[37,38] Other factors, such as possible metal toxicity, have been considered because nickel, in particular, is known to cause retinal necrosis in vivo.[39] However, based on a study of ion release from stainless steel into biofluids by Joseph et al. in 2009,[40] we find it unlikely that the very low levels of metal ions released over the time period, coupled with medium change every second day,

have any toxic effects. Thus, although the overall morphology of the magnet controls appears improved compared with standard cultures, the cell survival is not improved.

The underlying mechanism of stretch-related cell survival in the retina is not presently understood. Cell-membrane–bound stretch-activated ion channels have been identified in several tissues through which mechanical forces are sensed.[41] The channels open in response to membrane deformation, causing them to undergo a conformational change that allows ions to pass through. All types of stretch-activated ion channels respond to mechanical stimuli with a similar mechanism. Stiffness can also be regulated on both a cellular and ECM level through transcription factors such as YAP/TAZ, and this regulation appears to be dependent on the cell-to-substrate contact area.[42] This may be highly relevant in the context of retinal stretch. A multitude of sensory elements that respond to mechanical stimulation in vivo have been identified in the cornea, sclera, conjunctiva, lens, and uveal tract.[1,43–45] In the retina, direct mechanical stimulation of isolated tissue invokes ATP release, and a subsequent calcium ion wave propagation through the Müller cell network, resulting in Müller cell depolarization.[46] However, the mechanoreceptor responsible for this phenomenon has not yet been identified. One interesting candidate in this setting may be the transient receptor potential vanilloid 4 (TRPV4). TRPV4 has been shown to invoke responses to both understretch and overstretch through hyper- and hypo-osmolaric stress in chondrocytes.[47] Interestingly, Müller cells have also been shown to respond to hypo-osmotic stretch by calcium ion release mediated by this receptor, which in the retina is also expressed on ganglion cells.[48] Whether mechanical stretch activation in the retina is mediated by specific mechanoreceptors, as in many other tissues, remains to be elucidated.

In this study we have shown that lateral tension is an important factor for retinal cell survival. Stretched cultures displayed an overall preservation of the retinal architecture including sensitive structures such as photoreceptor inner and outer segments, an apparent lack of Müller cell activation, and an increased survival of ganglion cells and photoreceptors. These findings may provide a better understanding of ophthalmic diseases with an underlying mechanical pathogenesis.

References

1. Tan JCH, Coroneo MT. Are stretch-activated channels an ocular barometer? In: Kamkin A, Kiseleva I, eds. *Mechanosensitivity in Cells and Tissues. Vol. 2, Mechanosensitivity of the Nervous System*. New York: Springer-Verlag; 2008.
2. Eberhardt W, Woidich D, Reichenbach A. Determination of the extracellular tortuosity in nuclear layers of the central nervous system by resistance measurements on a geometrical model. *J Hirnforsch*. 1990;31:1–11.
3. Reichenbach A, Eberhardt W, Scheibe R, et al. Development of the rabbit retina. IV. Tissue tensility and elasticity in dependence on topographic specializations. *Exp Eye Res*. 1991;53:241–251.
4. Lindqvist N, Liu Q, Zajadacz J, Franze K, Reichenbach A. Retinal glial (Müller) cells: sensing and responding to tissue stretch. *Invest Ophthalmol Vis Sci*. 2010;51:1683–1690.
5. Wollensak G, Spoerl E. Biomechanical characteristics of the retina. *Retina*. 2004;24:967–970.
6. Lu YB, Franze K, Seifert G, et al. Viscoelastic properties of individual glial cells and neurons in the CNS. *Proc Natl Acad Sci U S A*. 2006;103:17759–17764.
7. Franze K, Francke M, Günter K, et al. Spatial mapping of the mechanical properties of the living retina using scanning force microscopy. *Soft Matter*. 2011;7:3147–3154.
8. Yao XY, Hageman GS, Marmor MF. Retinal adhesiveness in the monkey. *Invest Ophthalmol Vis Sci*. 1994;35:744–748.
9. Marmor MF, Yao XY, Hangeman GS. Retinal adhesiveness in surgically enucleated human eyes. *Retina*. 1994;14:181–186.
10. Fisher SK, Lewis GP, Linberg KA, Verardo MR. Cellular remodeling in mammalian retina: results from studies of experimental retinal detachment. *Prog Retin Eye Res*. 2005; 24:395–431.
11. Pastor JC, Méndez MC, de la Fuente MA, et al. Intraretinal immunohistochemistry findings in proliferative vitreoretinopathy with retinal shortening. *Ophthalmic Res*. 2006;38:193–200.
12. Levy J. Inherited retinal detachment. *Br J Ophthalmol*. 1952; 36:626–636.
13. Winkler J, Hagelstein S, Rohde M, Laqua H. Cellular and cytoskeletal dynamics within organ cultures of porcine neuroretina. *Exp Eye Res*. 2002;74:777–788.
14. García M, Forster V, Hicks D, Vecino E. Effects of Müller glia on cell survival and neuritogenesis in adult porcine retina in vitro. *Invest Ophthalmol Vis Sci*. 2002;43:3735–3743.
15. Caffé AR, Visser H, Jansen HG, Sanyal S. Histotypic differentiation of neonatal mouse retina in organ culture. *Curr Eye Res*. 1989;10:1083–1092.
16. Engelsberg K, Johansson K, Ghosh F. Development of the embryonic porcine neuroretina in vitro. *Ophthalmic Res*. 2005;37:104–111.
17. Engelsberg K, Ghosh F. Transplantation of cultured adult porcine neuroretina. *Cell Transplant*. 2007;16:31–39.
18. Kaempf S, Walter P, Salz AK, Thumann G. Novel organotypic culture model of adult mammalian neurosensory retina in co-culture with retinal pigment epithelium. *J Neurosci Methods*. 2008;17:47–58.
19. Kobuch K, Herrmann WA, Framme C, Sachs HG, Gabel VP, Hillenkamp J. Maintenance of adult porcine retina and retinal pigment epithelium in perfusion culture: characterisation of an organotypic in vitro model. *Exp Eye Res*. 2008;86:661–668.
20. Johansson UE, Eftekhari S, Warfvinge K. A battery of cell- and structure specific markers for the adult porcine retina. *J Histochem Cytochem*. 2010;58:377–389.
21. Galvin DJ, Watson RWG, Gillespie JI, Brady H, Fitzpatrick JM. Mechanical stretch regulates cell survival in human bladder smooth muscle cells in vitro. *Am J Physiol Renal Physiol*. 2002;283:1192–1199.
22. Springer AD, Hendrickson AE. Development of the primate area of high acuity 1: use of finite element analysis models to identify mechanical variables affecting pit formation. *Vis Neurosci*. 2004;21:53–62.
23. Ruggiero C, Benvenuti S, Giacomini M. Mathematical modeling of retinal mosaic formation by mechanical interactions and dendritic overlap. *IEEE Trans Nanobiosci*. 2007;6:180–185.
24. Fisher SK, Lewis GP. Müller cell and neuronal remodeling in retinal detachment and reattachment and their potential consequences for visual recovery: a review and reconsideration of recent data. *Vision Res*. 2003;43:887–897.
25. Sarthy V, Ripps H. *The Retinal Müller Cell: Structure and Function*. New York: Springer-Verlag; 2001.
26. Hauck SM, Suppmann S, Ueffing M. Proteomic profiling of primary retinal Müller glia cells reveals a shift in expression patterns upon adaptation to in vitro conditions. *Glia*. 2003;44: 251–263.
27. Bringmann A, Pannicke T, Grosche J, et al. Müller cells in the healthy and diseased retina. *Prog Retin Eye Res*. 2006;25:397–424.
28. Bringmann A, Iandiev I, Pannicke T, et al. Cellular signaling and factors involved in Müller cell gliosis: neuroprotective and detrimental effects. *Prog Retin Eye Res*. 2009;28:423–451.

29. Lu YB, Iandiev I, Hollborn M, et al. Reactive glial cells: increased stiffness correlates with increased intermediate filament expression. *FASEB J*. 2011;25:624–631.
30. Ghosh F, Johansson K. Neuronal and glial alterations in complex long-term rhegmatogenous retinal detachment. *Curr Eye Res*. 2012;37:704–711.
31. Wanner IB, Deik A, Torres M, et al. A new in vitro model of the glial scar inhibits axon growth. *Glia*. 2008;56:1691–1709.
32. Komaromy AM, Brooks DE, Kallberg ME, et al. Long-term effect of retinal ganglion cell axotomy on the histomorphometry of other cells in the porcine retina. *J Glaucoma*. 2003;12:307–315.
33. Davis JT, Wen Q, Janmey PA, Otteson DC, Foster WJ. Müller cell expression of genes implicated in proliferative vitreoretinopathy is influenced by substrate elastic modulus. *Invest Ophthalmol Vis Sci*. 2012;53:3014–3019.
34. da Costa BLSA, Kang KD, Rittenhouse KD, Osborne NN. The localization of PGE2 receptor subtypes in rat retinal cultures and the neuroprotective effect of the EP2 agonist butaprost. *Neurochem Int*. 2009;55:199–207.
35. Krishnamoorthy RR, Agarwal P, Prasanna G, et al. Characterization of a transformed rat retinal ganglion cell line. *Mol Brain Res*. 2001;86:1–12.
36. Fernandez-Bueno I, Pastor JC, Gayoso JM, Alcalde I, Garcia MT. Müller and macrophage-like cell interactions in an organotypic culture of porcine neuroretina. *Mol Vis*. 2008;14:2148–2156.
37. Cavopol AV, Wamil AW, Holcomb RR, McLean MJ. Measurement and analysis of static magnetic fields that block action potentials in cultured neurons. *Bioelectromagnetics*. 1995;16:197–206.
38. McLean MJ, Holcomb RR, Wamil AW, Pickett JD, Cavopol AV. Blockade of sensory neuron action potentials by a static magnetic field in the 10 mT range. *Bioelectromagnetics*. 2005;16:20–32.
39. Lauring L, Wergeland FL Jr. Ocular toxicity of newer industrial metals. *Mil Med*. 1970;135:1171–1174.
40. Joseph LA, Omoniyi IK, Ekanem EJ, Ekwumemgbo PA. Determination of metal ions released by stainless steel arch bar into bio-fluids. *Bull Chem Soc Ethiop*. 2009;23:37–45.
41. Sackin H. Stretch-activated ion channels. *Kidney Int*. 1995;48:1134–1147.
42. Dupont S, Morsut L, Aragona M, et al. Role of TAP/TAZ in mechanotransduction. *Nature*. 2011;474:179–183.
43. Belmonte C, Garcia-Hirschfeld J, Gallar J. Neurobiology of ocular pain. *Prog Retin Eye Res*. 1997;16:117–156.
44. Cooper KE, Tang JM, Rae JL, Eisenberg RS. A cation channel in frog lens epithelia responsive to pressure and calcium. *J Membr Biol*. 1986;93:259–269.
45. Mintenig GM, Sánchez-Vives MV, Martin C, Gual A, Belmonte C. Sensory receptors in the anterior uvea of the cat's eye. An in vitro study. *Invest Ophthalmol Vis Sci*. 1995;36:1615–1624.
46. Newman EA. Propagation of intracellular calcium waves in retinal astrocytes and Müller cells. *J Neurosci*. 2001;21:2215–2223.
47. Phan MN, Leddy HA, Votta BJ, et al. Functional characterization of TRPV4 as an osmotically sensitive ion channel in porcine articular chondrocytes. *Arthritis Rheum*. 2009;60:3028–3037.
48. Ryskamp DA, Witkovsky P, Barabas P, et al. The polymodal ion channel TRPV4 modulates calcium flux, spiking rate and apoptosis of mouse retinal ganglion cells. *J Neurosci*. 2011;31:7089–7101.
49. Khodair MA, Hagelstein S, Rohde M, Laqua H. Synaptic plasticity in mammalian photoreceptors prepared as sheets for retinal transplants. *Invest Ophthalmol Vis Sci*. 2003;44:4976–4988.